

Many body topological invariant, unitary preparation of Chern insulators and emergent bulk-boundary correspondence

Souvik Bandyopadhyay* and Amit Dutta

Department of Physics, Indian Institute of Technology Kanpur, Kanpur 208016, India

Utilising the non-uniqueness of the bulk macroscopic electrical polarisation in the topological phase of a Chern insulator, we construct a many body Chern invariant. Under a smooth unitary temporal evolution, this quantity evolves with time and successfully reflects the topology of the out-of-equilibrium state of the system by assuming an integer-quantised value in the *adiabatic* limit. Considering a linear ramping of the staggered Semenoff mass of the paradigmatic Haldane model of graphene, we illustrate that starting from a trivial state, it is indeed possible to obtain a topologically non-trivial state even by an adiabatic unitary driving protocol. We further propose a counter-diabatic protocol that enables us to suppress the diabatic excitations inevitable while crossing the gapless quantum critical point. The generalised topology of this dynamical Chern invariant being dependent on the non-equilibrium filling of single-particle states ensconces an emergent bulk-boundary correspondence that is expected to manifest in experiments.

There is a recent upsurge in studies of theoretical [1–18] and experimental [19–28] studies probing the generation and manipulation of topological phases of many body quantum systems. Such topological phases are characterized by different quantized values of a topological invariant which serves as a non-local order parameter characterizing the phases which are topologically inequivalent to each other. Distinct topological phases in thermodynamically large systems are necessarily separated by a quantum critical point (QCP) [29, 30]. Further, the extremely robust protection of topological phases against external local perturbations host an enormous multitude of possibilities of applications in topological quantum computation [31, 32] and controlling decoherence in out-of-equilibrium situations [33, 34].

Symmetry protected topological insulators (SPTs) (see [11–13], for review) and Chern insulators [14] host no long range topologically ordered states. Nevertheless the bulk topological non-triviality of SPTs and Chern insulators are manifested in the presence of topologically protected *boundary-localised* zero energy states when the bulk system is topologically non-trivial. This is the so-called bulk-boundary correspondence. Although the equilibrium topology of non-interacting quantum many body systems is well understood, comprehending the dynamical fate of equilibrium topology as well as characterising the topology of quantum systems which are driven out-of-equilibrium pose a challenging question of ongoing research [35–47]. The same is true concerning the emerging topology associated with dynamical quantum phase transitions [48, 49]

The success of designing a non-equilibrium topological system lies not only on the dynamical generation of a topological Hamiltonian [35, 37] but also on preparing the system in a topologically non-trivial dynamical state, e.g., in the ground state of the effective topological Hamiltonian. Despite several recent studies [50–59], the question whether the out-of-equilibrium state of a quantum many body system can be characterised by an integer-quantised topological index which is also mani-

festated in an emergent bulk-boundary correspondence is far from being settled.

Interestingly, for two-dimensional (2D) Chern insulating systems, a *no-go* theorem has been postulated [52], which states that the initial bulk topology of the model must not change under a smooth unitary transformation. This is an artefact of the temporal invariance of the dynamical bulk Chern number, constructed using the time evolved state of the system, under unitary driving. Nevertheless, following a quench the edge current eventually thermalizes to a value corresponding to the topology of the post-quench Hamiltonian [53–55]; thereby implying the absence of an out-of-equilibrium bulk-boundary correspondence. However, in Ref. [58] a stroboscopic "out-of-equilibrium" bulk-boundary correspondence has been established for 1D SSH and extended SSH models.

The question we address in this work is, whether it is possible to propose a generalised topological invariant which can characterise the out-of-equilibrium state of a Chern insulator, namely the Haldane model of graphene [14], under a smooth unitary evolution. We establish that it is indeed possible to define a generalised Chern number which, furthermore, changes dynamically and depending on time-dependent occupation of the eigenstates of the instantaneous Hamiltonian may assume an integer quantised value when the system is ramped from the non-topological to the topological phase. Considering an adiabatic ramping of the Semenoff mass of the Haldane model, we illustrate the above claim where we also propound a counter-diabatic (CD) protocol to suppress the non-adiabatic excitations. Furthermore, we explicitly demonstrate the emergence of an edge current and thus an emergent topological bulk-boundary correspondence.

We construct the generalised invariant, extending the equilibrium property of the non-uniqueness of the bulk electric polarisation in the topological phase of a Chern insulator to the non-equilibrium situation. To the best of our knowledge, the route, we unravel, to the unitary preparation of topological Chern insulators was not re-

ported before.

Macroscopic Electric Polarisation and Chern topology:

The macroscopic polarisation is in itself a many-body quantity. The generalised Chern number is conjectured using the property of non-uniqueness a component (say x) of macroscopic polarisation vector in the topological phase that fundamentally counts the winding of a uni-directional $U(1)$ connection along the other reciprocal lattice direction (i.e., along k_y). The branch singularity of the uni-directional Berry phase as a function of k_y then points to a non-zero value of the Chern number [60].

We evaluate the macroscopic electric polarisation vector of the system in the directions of the lattice vectors, $\vec{P} = \sum_i P_i \hat{i}$, where $P_i = \langle \hat{X}_i \rangle$, $\hat{X}_i = \sum_n x_i^n \hat{a}_n^\dagger \hat{a}_n$ is the many-body position operator and x_i^n denotes the i^{th} lattice direction of the n^{th} site with \hat{a}_n^\dagger being the creation operator of fermions. The expectation is here taken over the many-body state of the system. The translation operator in the i^{th} direction under periodic boundary conditions, $\hat{T}_i(\delta_i) = e^{i\delta_i \hat{X}_i}$, where we choose $\delta_i = 2\pi/N_i$, N_i being the linear dimension of the system in the i^{th} direction. Retaining only terms of linear order in δ_i (see [61]),

$$P_i[k_0] = \sum_\alpha \text{Im} \int_{BZ[k_0]} \langle \psi_{k,\alpha} | \partial_{k_i} | \psi_{k,\alpha} \rangle dk_x dk_y, \quad (1)$$

where k_0 is chosen to be the origin of the Brillouin zone (BZ) and $|\psi_{k,\alpha}\rangle$'s are the respective occupied single particle bands α . This is exactly the macroscopic polarisation of the system which is directly related to the integrated current flowing in the system under adiabatic evolution in Chern trivial phases.

However, in the Chern non-trivial (topological) phase, for every adiabatic shift in the origin of the BZ, the electric polarisation vector changes proportionally to the Chern invariant. If the system is in a pure state, for a shift in Δk_0 in the origin k_0 of the Brillouin zone,

$$P_i[k_0 + \Delta k_0] - P_i[k_0] = 2\pi \epsilon_{ij} (\Delta k_0)_j \mathcal{C}, \quad (2)$$

where \mathcal{C} is the Chern Number and ϵ_{ij} is the antisymmetric tensor. We utilize this non-uniqueness of the electric polarisation to define the Chern number as,

$$\mathcal{C} = \epsilon_{ij} \frac{\Delta P_i[k_0]}{2\pi \Delta k_{0j}}, \quad (3)$$

where $P_i[k_0]$ is as defined in Eq. (1).

Generalised Chern invariant under unitary dynamics:

We start from an initial eigenstate $|\psi(0)\rangle$ of a Chern insulator in the non-topological phase having $\mathcal{C} = 0$, which is subjected to an arbitrary unitary time dependent drive. To define the out-of-equilibrium Chern invariant, we extend the quantity defined in Eq. (1), to a weighted

average over the instantaneous single-particle bands (see [61]),

$$\tilde{P}_i = \sum_\alpha \text{Im} \int_{BZ} dk_x dk_y n_\alpha^k(t) A_i^k(|\phi_{k\alpha}(t)\rangle). \quad (4)$$

Here, $A_i^k(|\phi_{k\alpha}\rangle) = \langle \phi_{k\alpha} | \partial_{k_i} | \phi_{k\alpha} \rangle$ is the $U(1)$ gauge connection on the state $|\phi_{k\alpha}\rangle$ and the weights n_α^k are the time dependent population of the α^{th} instantaneous band.

We now proceed to define the dynamical Chern number as the change in the quantity \tilde{P}_i with a change of the BZ origin. This leads to the time-dependent Chern number,

$$\mathcal{C}^U(t) \propto \tilde{P}_x[k_0 + \Delta k_0] - \tilde{P}_x[k_0] = -\Delta k_{0y} \int_{k_{0y}}^{k_{0y}+1} dk_y \partial_{k_y} \beta(k_y, t), \quad (5)$$

where,

$$\beta(k_y, t) = -\sum_\alpha \text{Im} \int_{k_{0x}}^{k_{0x}+1} dk_x n_\alpha^k(t) A_i^k(|\phi_{k\alpha}(t)\rangle). \quad (6)$$

At *equilibrium*, when any one of the bands is completely filled, the quantity \tilde{P}_i , reduces to the total macroscopic polarisation of the occupied band. In this situation, the Chern number defined in Eq. (3) and (5) is defined as a gauge invariant quantity which simply detects a branch change of the function $\beta(k_y)$ in the closed interval $k_y \in [0, 1] \equiv \mathcal{S}^1$. By fixing a gauge, such that the quantity $\beta(k_y)$ remains continuous for all $k_y \in [0, 1]$, in a Chern non-trivial phase the function $\beta(k_y, t)$ exhibits a branch change at the endpoints of Brillouin zone,

$$\mathcal{C} \propto \beta(k_y + 1) - \beta(k_y). \quad (7)$$

Even under an arbitrary gauge choice, the existence of a branch singularity in the map $k_y \in [0, 1] \rightarrow \beta(k_y)$ signals the Chern non-triviality of the system. To elaborate, the sudden jump Δ in the $\beta(k_y)$ function in a non-trivial phase must be integer multiples of 2π where the integer multiple being the Chern number itself, precisely characterizes the homotopy class of the map, i.e.,

$$\Delta = -2\pi \mathcal{C}, \quad \mathcal{C} \in \mathcal{I}. \quad (8)$$

For a general *out-of-equilibrium* situation, the quantity $\mathcal{C}^U(t)$ defined in Eq. (5) fails to capture the $U(1)$ gauge connection of the time-evolved quantum state as a single instantaneous band may not be completely occupied far from equilibrium [62]. Nonetheless, for an *adiabatic* protocol dynamically exchanging the Chern character of the two bands, the $U(1)$ connection is over the many body projected band i.e., the instantaneous band which is nearly completely filled. This allows for the Chern number to vary in time. Thus, in the perfectly adiabatic situation, the macroscopic polarisation assumes the exact $U(1)$ form,

$$\tilde{P}_i = \text{Im} \int_{BZ} dk_x dk_y A_i^k(|\phi_{ks}(t)\rangle), \quad (9)$$

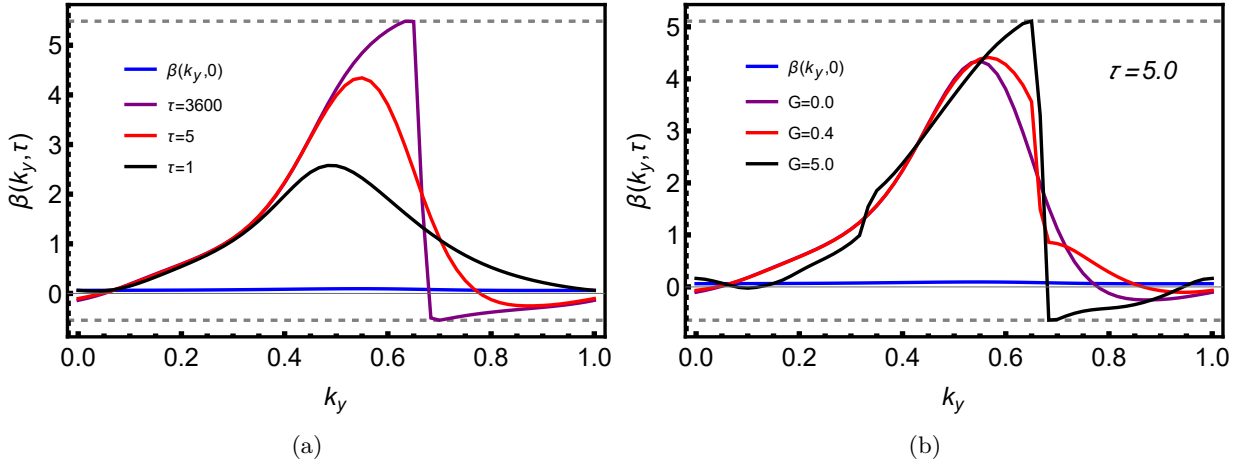


Figure 1: (a) Emergence of a sharp branch singularity in the function $\beta(k_y, \tau)$. The sharp jump in the $\beta(k_y, \tau)$ function for an adiabatic driving protocol (Eq. (10)) starting from an initial trivial state, demonstrates the topological non-triviality of the final time evolved state. The magnitude of the jump shown by the distance between the horizontal dashed lines is $\Delta = -0.96 \times 2\pi$. The initial and the final Hamiltonian is chosen such that, $t = 1.0$, $t_2 = 0.5$, $\phi = \pi/4$, $M_i = 3\sqrt{3}t_2 + 2.5$, $M_f = 3\sqrt{3}t_2 - 2.5$. (b) The $\beta(k_y, \tau)$ function exhibits a sharp branch singularity in the post-quench state for a drive employing shortcut to adiabaticity (Eqs. (11)-(12)) with increasing control field strength G . The magnitude of the jump shown by the distance between the horizontal dashed lines is $\Delta = -0.92 \times 2\pi$ with the set of quench parameters as in (a). The quenching period is chosen to be $\tau = 5.0$ which is much shorter than the adiabatic time scale ($\tau \simeq 3600$). Periodic boundary conditions are imposed with a grid size of 60×60 lattice sites in both the figures.

over the filled band $\alpha = s$.

The motivation behind incorporating the non-equilibrium occupations in Eq. (4) is the following: the topological classification of out of equilibrium states is directly connected to the evolution of particle currents generated in the time dependent state of the system. For the topological invariant to conform with the adiabatic edge current dynamics, it is essential to take note of the time evolution of the current operator. The measured current depends on the instantaneous Hamiltonian [52, 61, 63].

Illustration with Haldane model: To exemplify, we linearly quench the Semenoff mass ([61]),

$$H^k(t) = h_x \sigma_x + h_y \sigma_y + h_z(t) \sigma_z, \quad \text{with} \quad (10)$$

$$M(t) = M_i - (M_i - M_f) \frac{t}{\tau},$$

in time t . Initially ($t = 0$), the system is in a pure state $|\psi_k(0)\rangle$ which is the ground state of the initial (non-topological) Hamiltonian $H^k(0)$ and at $t = \tau$, the final value $M = M_f$ corresponds to a topological Hamiltonian; thus, the system is ramped across a QCP during the evolution.

We evaluate the function $\beta(k_y, t)$ at every instant of time in the time-dependent state $|\psi_k(t)\rangle$ generated following the evolution under the protocol in Eq. (10). As shown in Fig. 1a the function $\beta(k_y, t)$ evaluated on the circle $k_y \in [0, 1]$ develops a sharp branch singularity with

nearly quantized integral multiple of 2π , at the end of the quench $t = \tau$, only when the quench approaches the adiabatic limit. As discussed above, the existence of this sharp branch shift in $\beta(k_y, \tau)$, signals the topological non-triviality of the final state of the system.

Counter-diabatic protocol: During the passage through a gapless QCP, the adiabaticity criteria necessarily breaks down in the thermodynamic limit and diabatic excitations are inevitable. Nevertheless, the application of a control perturbation [63–65] may open up a gap even at the QCPs guaranteeing adiabaticity throughout the evolution, thereby, allowing for a much more efficient preparation of a topological state. The protocol we propose is the following:

$$H^k(t) = h_x \sigma_x + h_y \sigma_y + h_z(t) \sigma_z + B_x(t) \sigma_x \quad (11)$$

$$M(t) = M_i - (M_i - M_f) \frac{t}{\tau},$$

where the control (counter-diabatic) field is chosen as:

$$B_x(t) = G \sin\left(\frac{\pi t}{\tau}\right), t \in [0, \tau]; B_x(0) = B_x(\tau) = 0. \quad (12)$$

Again the initial system is in a trivial state while the final is expected to be topological one. Starting from the ground state of the initial Hamiltonian we probe the emergence of topology in the out of equilibrium state. In Fig. 1b, we observe that again the post-quench state develops a sharp branch singularity however in a much

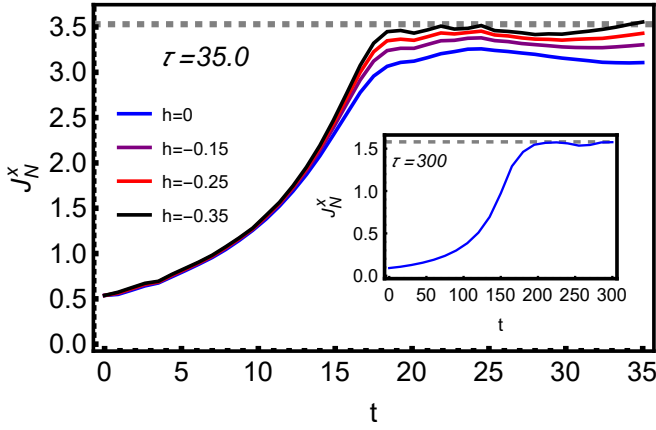


Figure 2: The time evolution of the current J_N^x through an arm-chair edge of the Haldane model with semi-open boundary conditions (periodic about the y-direction and open in x-direction) under a linear quench with the counter diabatic mass generation as in Eq. (11) with $t = 2.0$, $t_2 = 1.0$, $\phi = \pi/4$, $M_i = 3\sqrt{3}t_2 + 2.5$, $M_f = 0$, and the system size 18×18 lattice. h is the strength of the anisotropy introduced in the real space lattice generating the CD mass. (Inset) The adiabatic evolution of the edge-current vide the protocol in Eq. 10 with initial and final parameters same as in Fig. 1a for a 16×16 lattice. At the end of the quench, the edge-current (solid curve) indeed thermalizes to its equilibrium topological value (dashed line) in both protocols.

shorter duration of quench than that in the case of a perfectly adiabatic protocol. Moreover, the magnitude of the jump Δ is higher so that $C^U(\tau) \simeq 1$.

Bulk-boundary correspondence: The topological nature of the post quench state is manifested in the emergence of localized edge currents J_N^x under semi-periodic boundary conditions in a system having $N \times N$ atoms, as demonstrated in Fig. 2. The CD mass in Eq. (11) can be generated through an anisotropic strain [66, 67] in the real space lattice which in turn induces an anisotropy in the nearest neighbour hopping strength [61].

In conclusion, we have achieved the dynamical preparation of topological states of a Chern insulator within a unitary set up. The dynamical Chern number evolves with time unlike that defined in Ref. [52] and assumes an integer-quantised value for a perfectly adiabatic protocol. Starting with the ground state of the trivial Haldane Hamiltonian, we illustrate the emergence of a sharp branch singularity in the weighted average of the unidirectional Berry phase confirming that the evolved final state is indeed topological. This is further corroborated by an emergent bulk-boundary correspondence. The CD field we use to suppress diabatic excitations, can be

experimentally generated in graphene and borophene lattices by applying anisotropic strains in particular bond directions or through dynamical gap manipulations as explored theoretically and experimentally in [68–72].

We acknowledge Arijit Kundu, Anatoli Polkovnikov, Diptiman Sen, Sougato Mardanya and Utso Bhattacharya for helpful discussions and critical comments. We acknowledge Sourav Bhattacharjee and Somnath Maity for discussions. SB acknowledges PMRF, MHRD India for financial assistance. AD acknowledges financial support from SPARC program, MHRD, India. We also acknowledge ICTS, Bangalore, India where some part of the work was done.

* souvik@iitk.ac.in

- [1] A. Kitaev, Phys.-Usp. **44**, 131 (2001).
- [2] C. L. Kane and E. J. Mele, Phys. Rev. Lett. **95**, 226801 (2005).
- [3] B. A. Bernevig, T. L. Hughes, S.-C. Zhang, Science, **314**, 5806 (2006).
- [4] L. Fu and C. L. Kane, Phys. Rev. Lett. **100**, 096407 (2008).
- [5] C. W. Zhang, S. Tewari, R. M. Lutchyn, and S. Das Sarma, Phys. Rev. Lett. **101**, 160401 (2008).
- [6] M. Sato, Y. Takahashi, and S. Fujimoto, Phys. Rev. Lett. **103**, 020401 (2009).
- [7] J. D. Sau, R. M. Lutchyn, S. Tewari, and S. Das Sarma, Phys. Rev. Lett. **104**, 040502 (2010).
- [8] J. D. Sau, S. Tewari, R. M. Lutchyn, T. D. Stanescu, and S. Das Sarma, Phys. Rev. B **82**, 214509 (2010).
- [9] R. M. Lutchyn, J. D. Sau, and S. Das Sarma, Phys. Rev. Lett. **105**, 077001 (2010).
- [10] Y. Oreg, G. Refael, and F. von Oppen, Phys. Rev. Lett. **105**, 177002 (2010).
- [11] J. E. Moore, Nature **464**, 194 (2010).
- [12] S.-Q. Shen, *Topological Insulator*, Springer (2012).
- [13] B. A. Bernevig with T. L. Hughes, *Topological Insulators and Topological Superconductors*, Princeton University Press, Princeton (2013).
- [14] F. D. M. Haldane, Phys. Rev. Lett. **51**, 605 (1983).
- [15] X.G. Wen, Adv. Phys. **44**, 405 (1995).
- [16] A. Kitaev, Annals of Physics, **303**, Issue 1, (2003).
- [17] A. Kitaev, Annals of Physics, **321**, Issue 1 (2006).
- [18] M. Levin and X.G. Wen, Phys. Rev. Lett. **96**, 110405 (2006).
- [19] V. Mourik, K. Zuo, S. M. Frolov, S. R. Plissard, E. P. A. M. Bakkers, and L. P. Kouwenhoven, Science **336**, 1003 (2012).
- [20] L. P. Rokhinson, X. Liu, and J. K. Furdyna, Nat. Phys. **8**, 795 (2012).
- [21] M. T. Deng, C. L. Yu, G. Y. Huang, M. Larsson, P. Caroff, and H. Q. Xu, Nano Lett. **12**, 6414 (2012).
- [22] A. Das, Y. Ronen, Y. Most, Y. Oreg, M. Heiblum, and H. Shtrikman, Nat. Phys. **8**, 887 (2012).
- [23] H. O. H. Churchill, V. Fatemi, K. Grove-Rasmussen, M. T. Deng, P. Caroff, H. Q. Xu, and C. M. Marcus, Phys. Rev. B **87**, 241401(R) (2013).
- [24] A. D. K. Finck, D. J. Van Harlingen, P. K. Mohseni, K.

- Jung, and X. Li, Phys. Rev. Lett. **110**, 126406 (2013).
- [25] J. Alicea, Rep. Prog. Phys. **75**, 076501 (2012).
- [26] M. Leijnse and K. Flensberg, Semicond. Sci. Technol. **27**, 124003 (2012).
- [27] C. W. J. Beenakker, Annu. Rev. Con. Mat. Phys. **4**, 113 (2013).
- [28] T. D. Stanescu and S. Tewari, J. Phys.: Condens. Matter **25**, 233201 (2013).
- [29] S. Sachdev, *Quantum Phase Transitions*, Cambridge University Press, Cambridge (2010).
- [30] A. Dutta, G. Aeppli, B. K. Chakrabarti, U. Divakaran, T. F. Rosenbaum, D. Sen, *Quantum Phase Transitions in Transverse Field Spin Models*, Cambridge University Press, Cambridge (2015).
- [31] A. Kitaev and C. Laumann, arXiv:0904.2771, (2016).
- [32] V. Lahtinen, J. K. Pachos, SciPost Phys. **3**, 021 (2017).
- [33] B. Damski, H. T. Quan, W. H. Zurek Phys. Rev. A **83**, 062104, (2011).
- [34] T Nag, U Divakaran, A Dutta, Phys. Rev. B **86**, 020401. (2012).
- [35] T. Oka and H. Aoki, Phys. Rev. B **79**, 081406 (R) (2009).
- [36] A. Bermudez, D. Patane, L. Amico, and M. A. Martin Delgado, Phys. Rev. Lett. **102**, 135702 (2009).
- [37] T. Kitagawa, T. Oka, A. Brataas, L. Fu, and E. Demler, Phys. Rev. B **84**, 235108 (2011).
- [38] N. H. Lindner, G. Refael, and V. Galitski, Nat. Phys. **7**, 490 (2011).
- [39] A. A. Patel, S. Sharma, and A. Dutta, Eur. Phys. J. B **86**, 367 (2013).
- [40] A Rajak, A Dutta, Phys. Rev. E **89**, 042125 (2014).
- [41] M. Thakurathi, A. A. Patel, D. Sen, and A. Dutta, Phys. Rev. B **88**, 155133 (2013).
- [42] A. Kundu and B. Seradjeh, Phys. Rev. Lett. **111**, 136402 (2013).
- [43] J. Cayssol, B. Dora, F. Simon, and R. Moessner, Phys. Status Solidi RRL **7**, 101 (2013).
- [44] M.S. Rudner, N.H. Lindner, E. Berg, and M. Levin, Phys. Rev. X **3**, 031005 (2013).
- [45] L. E. F. Foa Torres, P. M. Perez-Piskunow, C. A. Balseiro, and G. Usaj, Phys. Rev. Lett. **113**, 266801 (2014).
- [46] H. Dehghani, T. Oka, and A. Mitra, Phys. Rev. B **91**, 155422 (2015).
- [47] J.H. Wilson, J. C.W. Song, and G. Refael, Phys. Rev. Lett. **117**, 235302 (2016).
- [48] J.C. Budich and M. Heyl, Phy. Rev. B **93**, 085416 (2016).
- [49] U Bhattacharya, A Dutta, Phys. Rev. B **96**, 014302 (2017).
- [50] M. S. Foster, M. Dzero, V. Gurarie, and E. A. Yuzbashyan, Phys. Rev. B **88**, 104511 (2013).
- [51] M. S. Foster, V. Gurarie, M. Dzero, and E. A. Yuzbashyan, Phys. Rev. Lett. **113**, 076403 (2014).
- [52] L. D'Alessio and M. Rigol, Nature Communications **6**, 8336 (2015).
- [53] M.D. Caio, N.R. Cooper, and M.J. Bhaseen, Phys. Rev. Lett. **115**, 236403 (2015).
- [54] U. Bhattacharya, J. Hutchinson, and A. Dutta, Phys. Rev. B **95**, 144304 (2017).
- [55] S. Mardanya, U. Bhattacharya, A. Agarwal, and A. Dutta, Phys. Rev. B **97**, 115443 (2018).
- [56] M. McGinley and N.R. Cooper, Phys. Rev. Lett. **121**, 090401 (2018).
- [57] S. Bandyopadhyay, U. Bhattacharya and A. Dutta, Phys. Rev. B **100**, 054305 (2019).
- [58] S. Bandyopadhyay and A. Dutta, Phys. Rev. B **100**, 144302 (2019).
- [59] L. Pastori, S. Barbarino, and J. C. Budich, arXiv:2003.07874 (2020).
- [60] S. Coh and D. Vanderbilt, Phys. Rev. Lett. **102**, 107603 (2009).
- [61] Supplemental Material
- [62] This is reflected in the weighted sum β defined in Eq. (6), as it is no longer quantized on the boundaries of the S^1 loop $k_y \in [0, 1]$.
- [63] M. Bukov and A. Polkovnikov, Phys. Rev. A **90**, 043613 (2014).
- [64] D. Sels and A. Polkovnikov, Proc. Natl. Acad. Sci. U.S.A. **114**, E3909 (2017).
- [65] P.W. Claeys, M. Pandey, D. Sels, and A. Polkovnikov, Phys. Rev. Lett. **123**, 090602 (2019).
- [66] V.M. Pereira, A.H. Castro Neto, Phys. Rev. Lett. **103**, 046801 (2009).
- [67] M. R. Masir, D. Moldovan, and F. M. Peeters, Solid State Commun. **175-176**, 76 (2013).
- [68] M.O. Leyva and G.G. Naumis, Phys. Rev. B **93**, 035439 (2016).
- [69] M.O. Leyva and G.G. Naumis, Phys. Rev. B **88**, 085430 (2013).
- [70] H.T. Yang, J. Phys.: Condens. Matter **23** 505502 (2011).
- [71] N. Levy *et.al.*, Science **329**, 5991 (2010).
- [72] V.G.I. Sierra, J.C.S. Santana, A. Kunold, and G.G. Naumis, Phys. Rev. B **100**, 125302 (2019).

Supplemental Material on “Many body topological invariant, unitary preparation of Chern insulators and emergent bulk-boundary correspondence”

A BRIEF REVIEW ON HALDANE MODEL OF GRAPHENE :

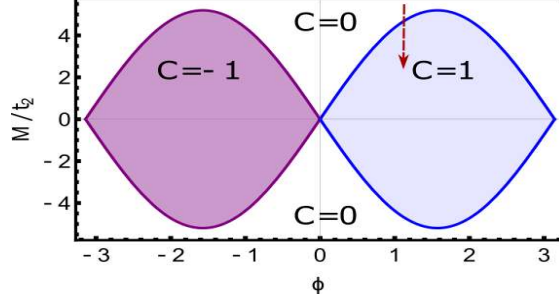


Figure S1: (Color online) The topological phase diagram of the Haldane model. The distinct topological phases are separated by quantum critical lines on which the parameter values are such that the system becomes gapless. The parameter regions showing non-zero values of the Chern number (C) are topologically non-trivial. The red arrow show the direction and the initial and final region of the quench employed in the manuscript.

The bare Hamiltonian for the Haldane model [S1] is obtained by breaking the time reversal and sublattice of graphene ,

$$H_{\alpha,\beta,n,m}^0 = -t_1 \sum_{\langle m\alpha,n\beta \rangle} a_{m,\alpha}^\dagger a_{n,\beta} + M \sum_n a_{n,A}^\dagger a_{n,A} - M \sum_n a_{n,B}^\dagger a_{n,B} - \sum_{\langle\langle m\alpha,n\alpha \rangle\rangle} t_2 e^{i\phi} a_{m,\alpha}^\dagger a_{n,\alpha} + h.c., \quad (S1)$$

where the real nearest neighbour (N1) hopping t_1 (with $t_2 = 0, M = 0$) comprises the bare graphene Hamiltonian; the indices n and α represent site and sublattice respectively. The diagonal staggered mass (Semenoff mass) M explicitly breaks the sublattice symmetry of the model. Further the complex next nearest neighbour (N2) hopping term t_2 , is applied such that the time reversal symmetry is broken in the next nearest neighbour hopping while the net flux through each plaquette remains zero. The Haldane model is known to exhibit non-trivial Chern topology when its ground state is completely filled depending on the parameters M, t_1, t_2 and ϕ .

Interestingly, the Haldane model with explicitly broken time reversal symmetry is known to host topologically non-trivial phases for certain parameter regions. The topology of the Hamiltonian is essentially the homotopy classification of the map $(k_x, k_y) \rightarrow H^k(k_x, k_y)$ in reciprocal space and is characterized by the gauge invariant Chern topological invariant,

$$C = \frac{1}{(2\pi)^2} \int_{BZ} dk_x dk_y \mathcal{F}_{xy}(|\psi_k\rangle), \quad (S2)$$

where, $\mathcal{F}_{xy}(|\psi_k\rangle)$ is the berry curvature defined over the ground state $|\psi_k\rangle$ of the Hamiltonian H^k , i.e.,

$$\mathcal{F}_{xy}(|\psi_k\rangle) = \partial_{k_x} \langle \psi_k | \partial_{k_y} | \psi_k \rangle - \partial_{k_y} \langle \psi_k | \partial_{k_x} | \psi_k \rangle. \quad (S3)$$

The Chern invariant is integer quantized as long as the Hamiltonian H^k does not approach a QCP where the Chern number becomes ill-defined. Different integer values of the Chern number characterize distinct topological phases separated by QCPs (see Fig. S1).

Each point on the Bravais lattice can be referenced in terms of the Bravais lattice vectors, i.e.,

$$\vec{a} = n_x \vec{a}_x + n_y \vec{a}_y, \quad (S4)$$

where the vectors \vec{a}_x and \vec{a}_y span the Bravais lattice and n_x, n_y are integers. We choose the vectors \vec{a}_x and \vec{a}_y to be the next nearest neighbour hopping vectors such that,

$$\begin{aligned} \vec{a}_x &= \vec{\Delta}_{22}, \\ \vec{a}_y &= -\vec{\Delta}_{21}, \end{aligned} \quad (S5)$$

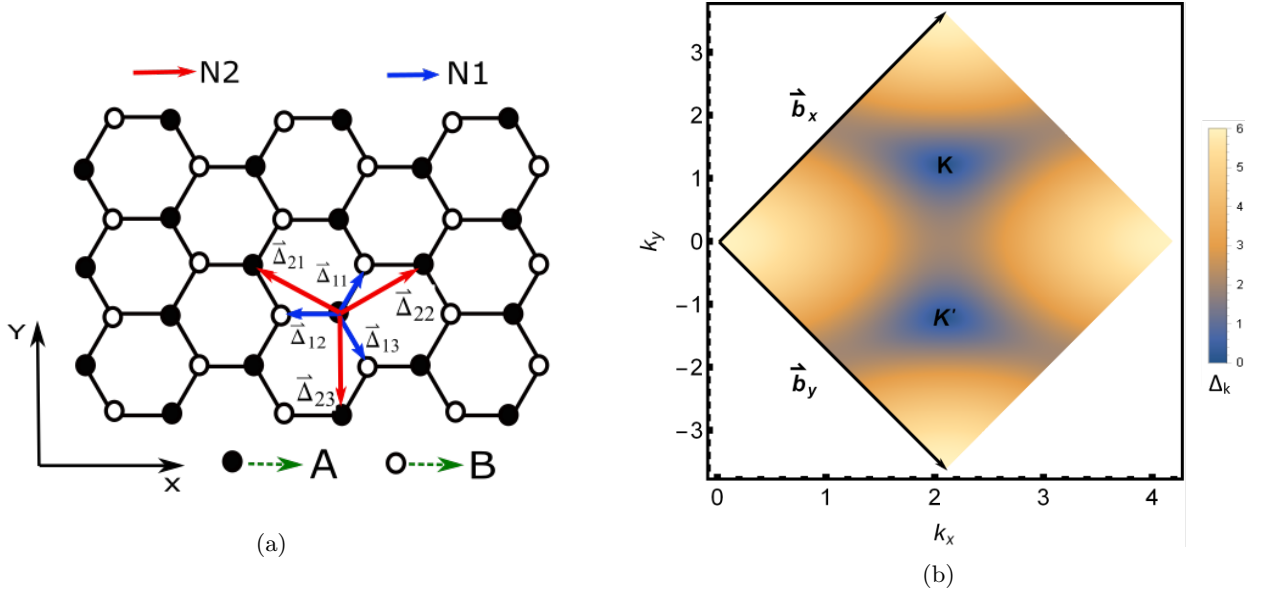


Figure S2: (Color online) (a) The hexagonal graphene lattice showing the nearest neighbour (N1) and next-nearest neighbour (N2) hopping vectors $\vec{\Delta}_{1i}$ and $\vec{\Delta}_{2i}$, respectively, where the lattice constant is set to be $a = 1$. The hollow and the filled atoms represent the B and A sublattices respectively. (b) The Brillouin zone of graphene containing two inequivalent Dirac points K and K' . The color density shows the absolute value of the bandgap Δ_k of the reciprocal space graphene Hamiltonian showing vanishing gaps at the Dirac points for a 600×600 lattice size having the N1 hopping strength $t = 1.0$ and the N2 hopping $t_2 = 0$.

where $\vec{\Delta}_{2i}$ are the N2 vectors as shown in Fig. S2a.

Invoking the discrete translational invariance of the Hamiltonian one can employ a discrete Fourier transform to decouple the Hamiltonian $H(t)$ in momentum space. The reciprocal space is spanned by the reciprocal lattice vectors \vec{b}_x and \vec{b}_y , i.e. every reciprocal lattice point can be represented as,

$$\vec{b} = k_x \vec{b}_x + k_y \vec{b}_y, \quad (S6)$$

where, $k_x, k_y \in [0, 1)$. We choose a rhomboidal Brillouin zone spanned by reciprocal lattice vectors \vec{b}_x and \vec{b}_y (see Fig. S2b) containing two independent Dirac points K and K' . In our choice of representation,

$$\vec{b}_x = \frac{2\pi}{3a} \{1, \sqrt{3}\} \quad \text{and} \quad \vec{b}_y = \frac{2\pi}{3a} \{1, -\sqrt{3}\}, \quad (S7)$$

where we have chosen $a = 1$. The corresponding inequivalent Dirac points in the Brillouin zone shown in Fig. S2b are given by,

$$K = \frac{2\pi}{3} \left(1, \frac{1}{\sqrt{3}}\right) \quad \text{and} \quad K' = \frac{2\pi}{3} \left(1, -\frac{1}{\sqrt{3}}\right). \quad (S8)$$

The bare Haldane Hamiltonian gets decoupled in the momentum space where $H^0(k)$ can be written in the basis $|k, A\rangle$ and $|k, B\rangle$ as,

$$H^0(k) = \vec{h}(k) \cdot \vec{\sigma} = h_x(k) \sigma_x + h_y(k) \sigma_y + h_z(k) \sigma_z, \quad (S9)$$

such that,

$$\begin{aligned}
h_x(k) &= -t \sum_{i=1}^3 \cos(\vec{k} \cdot \vec{\Delta}_{1i}), \\
h_y(k) &= -t \sum_{i=1}^3 \sin(\vec{k} \cdot \vec{\Delta}_{1i}), \\
h_z(k) &= M - t_2 \sin \phi \sum_{i=1}^3 \sin(\vec{k} \cdot \vec{\Delta}_{2i}),
\end{aligned} \tag{S10}$$

$\vec{\Delta}_{1i}$ and $\vec{\Delta}_{2i}$ are the nearest neighbour and next nearest neighbour lattice vectors respectively (see Fig. S2a) chosen to be,

$$\begin{aligned}
\vec{\Delta}_{11} &= \frac{a}{2}\{1, \sqrt{3}\}, \quad \vec{\Delta}_{12} = \{-a, 0\}, \quad \vec{\Delta}_{13} = \frac{a}{2}\{1, -\sqrt{3}\} \quad \text{and}, \\
\vec{\Delta}_{21} &= \frac{a}{2}\{-3, \sqrt{3}\}, \quad \vec{\Delta}_{22} = \frac{a}{2}\{3, \sqrt{3}\}, \quad \vec{\Delta}_{23} = \{0, -a\sqrt{3}\},
\end{aligned} \tag{S11}$$

in the cartesian frame (Fig. S2a) where we have chosen the lattice parameter $a = 1$. Note that we have used Eq. (S9) in Eq. (15) of the main text where the Semenoff mass term which appears only in $h_z(k)$ is linearly ramped across the quantum critical point from the non-topological to the topological phase.

MACROSCOPIC POLARISATION AND ITS OUT-OF-EQUILIBRIUM GENERALISATION

We evaluate the macroscopic electric polarisation vector [S2] of the system in the directions of the lattice vectors (Eq. (S5) and Fig. S2a),

$$\vec{P} = \sum_i P_i \hat{i}, \tag{S12}$$

where $P_i = \langle \hat{X}_i \rangle$, $\hat{X}_i = \sum_n x_i^n \hat{a}_n^\dagger \hat{a}_n$ is the many-body position operator and x_i^n denotes the i^{th} coordinate of the n^{th} site. The expectation is taken over a fermionic many body state. The translation operator in the i^{th} direction under periodic boundary conditions,

$$\hat{T}_i(\delta_i) = e^{i\delta_i \hat{X}_i}, \tag{S13}$$

where we choose $\delta_i = 2\pi/N_i$, N_i being the dimension of the system in the i^{th} direction. The periodicity of the exponential enforces periodic boundary conditions on the lattice. Therefore, under periodic boundary conditions and in the thermodynamic limit, the macroscopic polarisation of the system assumes the following form,

$$P_i = \text{Im} \ln \langle \hat{T}_i \rangle, \tag{S14}$$

where the expectation is taken over the full many-body state of the system. In the thermodynamic limit, this compactified definition of the macroscopic polarisation reduces to the conventional bulk polarisation of the system. This is evident from the fact that, for a many-particle pure state, $|\Psi\rangle$ (which is a slater determinant of the occupied single-particle states),

$$P_i = \text{Im} \ln \langle \hat{T}_i \rangle = \text{Im} \ln \det U = \text{Im} \ln e^{\text{Tr} \ln U}, \tag{S15}$$

where the matrix U contains all the overlap of the single-particle matrix T_i between the occupied single particle states, i.e.,

$$U_{mn} = \langle \psi_m | T_i | \psi_n \rangle \implies (U)_{k\alpha, k'\beta} = \langle \psi_{k_i+\delta_i, \alpha} | \psi_{k, \alpha} \rangle \simeq e^{-i(A_i^k)_{\alpha\alpha} \delta_i}, \tag{S16}$$

where k denotes the single-particle momenta while α and β are the band indices and $(A_i^k)_{\alpha\alpha}$ is the $U(1)$ connection of the α^{th} occupied band. In the thermodynamic limit ($\delta_i \rightarrow 0$), retaining only terms of linear order in δ_i , one obtains,

$$P_i = \sum_{\alpha} \text{Im} \int_{BZ} \langle \psi_{k,\alpha} | \partial_{k_i} | \psi_{k,\alpha} \rangle dk_x dk_y, \quad (\text{S17})$$

which is the macroscopic polarisation of the system.

In the main text, we consider an arbitrary unitary drive starting from an initial eigenstate state $|\psi(0)\rangle$ of the Chern insulator (this ensures half-filling of the initial single-particle states) in the non-topological phase with $\mathcal{C} = 0$ (as shown in Fig. S1) such that the time evolved state is,

$$|\psi(t)\rangle = U(t, 0) |\psi(0)\rangle, \quad (\text{S18})$$

where $U(t, 0)$ is the evolution operator generated by an instantaneous hermitian Hamiltonian $H(t)$. Translating to Fourier space, the instantaneous eigenmodes $|\phi_{k\alpha}(t)\rangle$ of the instantaneous Hamiltonian $H_k(t)$ satisfy,

$$H_k(t) |\phi_{k\alpha}(t)\rangle = E_{k\alpha}(t) |\phi_{k\alpha}(t)\rangle, \quad (\text{S19})$$

with eigenvalues $E_{k\alpha}(t)$, for all $k \in BZ$. and α denotes the band index.

As discussed in Eq. (S17), the electric polarisation in the i^{th} direction for an arbitrary pure quantum many-body state $|\chi\rangle$ reduces to the average of the quantity,

$$\Lambda_i^k = \sum_{\alpha} A_i^k(|\chi_{k\alpha}\rangle), \quad (\text{S20})$$

over the complete Brillouin zone and summed over all the occupied single particle states $|\chi_{k\alpha}\rangle$. Here, $A_i^k(|\chi_{k\alpha}\rangle)$ is the $U(1)$ gauge connection on the state $|\chi_{k\alpha}\rangle$ i.e.,

$$A_i^k(|\chi_{k\alpha}\rangle) = \langle \chi_{k\alpha} | \partial_{k_i} | \chi_{k\alpha} \rangle. \quad (\text{S21})$$

In the out-of-equilibrium situation, we extend the quantity defined in Eq. (S17) as a weighted average over the instantaneous single-particle bands,

$$\tilde{P}_i = \sum_{\alpha} \text{Im} \int_{BZ} dk_x dk_y n_{\alpha}^k(t) A_i^k(|\phi_{k\alpha}(t)\rangle), \quad (\text{S22})$$

where the weights $n_{\alpha}^k(t)$ are the time dependent population of the α^{th} instantaneous band i.e.,

$$n_{\alpha}^k(t) = \langle \psi_k(t) | c_{k\alpha}^{\dagger}(t) c_{k\alpha}(t) | \psi_k(t) \rangle, \quad (\text{S23})$$

where $c_{k\alpha}(t)$ and $c_{k\alpha}^{\dagger}(t)$ are the annihilation and creation operators respectively, of the eigenmodes of the instantaneous Hamiltonian $H_k(t)$, i.e., $c_{k\alpha}^{\dagger}(t) |0\rangle = |\phi_{k\alpha}(t)\rangle$, where $|0\rangle$ is fermionic vacuum. \tilde{P}_i is the weighted average of the electric polarisation in each band of the time-evolved Hamiltonian $H(t)$; the weights being precisely the time dependent population of each band.

CURRENTS

The definition of the topological classification of out of equilibrium states is directly connected to the evolution of particle currents generated in the time dependent state of the system. For the topological invariant to conform with the adiabatic edge current dynamics, it is essential to take note of the time evolution of the current operator.

As discussed in Refs. [S3, 4], the measured particle current in the out of equilibrium system is dependent on the instantaneous Hamiltonian. This can be easily seen by explicitly computing the expectation of the current operator between two sites when the system is driven out of equilibrium. Referring to the Haldane Hamiltonian and resorting to the Heisenberg picture,

$$\frac{d(a_n^{\dagger} a_m)}{dt} = -i [H(t), a_n^{\dagger} a_m]. \quad (\text{S24})$$

As the dynamics is unitary, the mean rate of change of local population at a site is directly proportional to the average local current at the site. Thus, the expectation,

$$\left\langle \frac{d(a_n^\dagger a_m)}{dt} \right\rangle = \sum_n J_{nm}, \quad (\text{S25})$$

where J_{nm} is the average current between the sites i and j . Comparing Eq. (S24) and Eq. (S25), one obtains,

$$J_{nm} = \text{Im} [2H_{nm}(t) \langle a_n^\dagger a_m \rangle], \quad (\text{S26})$$

where $H_{nm}(t)$ is the single particle time dependent Hamiltonian,

$$H(t) = \sum_{nm} H(t)_{nm} a_n^\dagger a_m, \quad (\text{S27})$$

. To evaluate the edge currents we impose semi-periodic boundary conditions on the 2D lattice. Generically, as defined above, the single particle current can be decomposed as,

$$\langle \vec{J}_{SS} \rangle = \langle \vec{J}_N \rangle + \langle \vec{J}_{NN} \rangle, \quad (\text{S28})$$

where \vec{J}_N and \vec{J}_{NN} are the nearest neighbour and the next nearest neighbour current operators respectively,

$$\begin{aligned} \langle J_{Nn}^x \rangle &= \sum_m t_1 \langle a_n^\dagger a_m \rangle - hc \\ \langle J_{NNn}^x \rangle &= \sum_m t_2 \langle a_n^\dagger a_m \rangle - hc, \end{aligned} \quad (\text{S29})$$

where $\langle J_{Nn}^x \rangle (\langle J_{NNn}^x \rangle)$ is the nearest(next nearest) current at the n^{th} site and the summation indices extends over all nearest (next-nearest) neighbour sites to the n^{th} site. Considering the lattice to be periodically wrapped in the x-direction (see Fig. S2a) while being open in the y-direction, one obtains two arm-chair edges at the ends of the cylinder. We compute the total horizontal current flowing in the periodic x-direction on one of the arm chair edges J_N^x for a $N \times N$ lattice, in the post quench state to re-establish the bulk boundary correspondence which is depicted in Fig. (2) of the main manuscript.

EXPERIMENTAL GENERATION OF THE COUNTER-DIABATIC MASS

The time-dependent generation of the counter-diabatic term in Eq. (11) of the main text can be realised experimentally by a temporal modulation of the nearest neighbour hopping amplitude along a particular direction in the real lattice. In Fig. (2) of the manuscript we explicitly demonstrate this by applying a time dependent modulation to the hopping strength along the direction $\vec{\Delta}_{12}$ while keeping the other two nearest-neighbour and next-nearest neighbour hoppings unaffected,

$$\begin{aligned} t_{\vec{\Delta}_{12}}(t) &= -t_1 - h \times \sin\left(\frac{\pi t}{\tau}\right) \\ t_{\vec{\Delta}_{11}} &= -t_1, \\ t_{\vec{\Delta}_{13}} &= -t_1, \end{aligned} \quad (\text{S30})$$

for the duration of the quench, i.e. $t \in [0, \tau]$. Such anisotropic modulations can be generated experimentally by applying anisotropic strain on the graphene lattice and then modifying it temporally to open up a controlled gap in the spectrum [S5, 6] which in turn suppresses diabatic excitations while crossing a quantum critical point.

* souvik@iitk.ac.in

[S1] F. D. M. Haldane, Phys. Rev. Lett. **51**, 605 (1983).

- [S2] S. Coh and D. Vanderbilt, Phys. Rev. Lett. **102**, 107603 (2009).
- [S3] L. D'Alessio and M. Rigol, Nature Communications **6**, 8336 (2015).
- [S4] M. Bukov and A. Polkovnikov, Phys. Rev. A **90**, 043613 (2014).
- [S5] V.M. Pereira, A.H. Castro Neto, Phys. Rev. Lett. **103**, 046801 (2009).
- [S6] M. R. Masir, D. Moldovan, and F. M. Peeters, Solid State Commun. **175-176**, 76 (2013).